

000 QUANTIZED CACHE-TO-CACHE: COMMUNICATION- 001 BUDGETED KV TRANSFER FOR HETEROGENEOUS 002 LLMS

006 **Anonymous authors**

007 Paper under double-blind review

011 ABSTRACT

013 We study communication-efficient transfer between heterogeneous large language
014 models (LLMs) by quantizing Cache-to-Cache (C2C) KV-cache transfer. Our
015 goal is to reduce bandwidth and memory while preserving accuracy. We present
016 post-training quantization (INT8/INT4), cache-length reduction, and accuracy-
017 versus-bytes curves for C2C, and introduce receiver-aware token selection and
018 rate-distortion mixed-precision scheduling for sparse transfer. Empirically, quan-
019 tization is nearly lossless, cache-length pruning reveals a strong front/back asym-
020 metry, and our delta-selection improves accuracy at fixed token budgets while RD
021 scheduling matches or improves accuracy at fixed byte budgets. We release a
022 reproducible evaluation pipeline and analysis scripts.

024 1 INTRODUCTION

027 Large language models (LLMs) often communicate via text, which is slow and lossy. Cache-to-
028 Cache (C2C) communicates via KV-cache projection and fusion, but does not address precision or
029 bandwidth constraints. We ask: *How low can KV precision go before accuracy collapses, and can*
030 *we recover performance under tight communication budgets?*

032 Contributions.

- 034 • We introduce a precision-aware C2C evaluation pipeline and quantify INT8/INT4 PTQ effects on
035 C2C accuracy.
- 037 • We study cache-length reduction as a second budget axis and show that back-pruning consistently
038 outperforms front-pruning.
- 039 • We report accuracy vs. communication-budget curves that jointly compare precision and cache
040 length.
- 041 • We propose receiver-aware delta token selection and rate-distortion token×precision scheduling
042 for sparse, budgeted C2C transfer.
- 044 • We provide a reproducible benchmarking setup and analysis scripts to support extensions to QAT,
045 mixed precision, heterogeneity, and selective transfer.

047 2 BACKGROUND AND MOTIVATION

050 C2C projects sharer KV caches into receiver space and fuses them with learned gates, preserving rich
051 semantics compared to text relay. However, KV caches are large: they scale with sequence length,
052 KV heads, and head dimension. Quantization and cache-length reduction can shrink the communi-
053 cation footprint while retaining accuracy. This work reframes C2C through a communication-budget
lens.

054 **3 RELATED WORK**

056 **C2C.** Cache-to-Cache (C2C) enables direct semantic communication by projecting and fusing a
 057 sharer model’s KV cache into a receiver’s KV cache with learnable gates, avoiding intermediate text
 058 generation (Fu et al., 2025).

059 **KV communication across agents.** KVComm aligns KV caches across diverging prefixes us-
 060 ing training-free offset correction with online anchors (Ye et al., 2025). Q-KVComm adds
 061 adaptive layer-wise quantization, hybrid information extraction, and heterogeneous calibration
 062 for compressed KV transfer (Kriuk & Ng, 2025). These works focus on multi-agent cache
 063 reuse/compression; our work studies quantization and cache-length pruning within the C2C pro-
 064 jector+fuser pipeline.

065 **Latent collaboration and cache alignment.** KV cache alignment learns a shared latent space with
 066 adapters to align KV caches across models (Dery et al., 2026). LatentMAS enables latent-space
 067 collaboration with shared working memory without extra training (Zou et al., 2025). Our approach
 068 stays within C2C’s KV fusion but emphasizes communication budgets and precision/length trade-
 069 offs.

070 **Token selection and KV compression.** Token-level KV selection and value-norm importance
 071 improve long-context inference for a single model (ZipCache, TokenSelect, VATP) (Anonymous,
 072 2024b; 2025; 2024a). We adopt the budget perspective for C2C rather than single-model KV com-
 073 pression.

075 **4 METHOD**

076 **4.1 C2C RECAP**

077 Let the sharer model produce KV caches (K_ℓ^S, V_ℓ^S) and the receiver produce (K_ℓ^R, V_ℓ^R) at layer ℓ .
 078 C2C projects sharer KV into receiver space via Π_ℓ^K, Π_ℓ^V and fuses them through a learnable gate:

$$(K_\ell^{R'}, V_\ell^{R'}) = \mathcal{F}_\ell(K_\ell^R, V_\ell^R, \Pi_\ell^K(K_\ell^S), \Pi_\ell^V(V_\ell^S)).$$

079 This avoids intermediate text and transfers richer internal semantics.

080 **4.2 POST-TRAINING QUANTIZATION (PTQ)**

081 We quantize the KV caches using INT8 or INT4/NF4 with per-head scaling. We evaluate accuracy
 082 and latency under fixed precision budgets. Our current implementation uses fake-quant (quantize
 083 then dequantize) to model quantization noise without bit-packing.

084 **4.3 CACHE-LENGTH REDUCTION**

085 We prune KV tokens using a fixed ratio (e.g., 50%, 25%, 10%), reducing transmitted bytes further.
 086 We evaluate front-pruning and back-pruning to diagnose which instruction tokens are most valuable
 087 for cross-model transfer.

088 **4.4 SELECTIVE AND COMPRESSED CACHE TRANSFER (SPARSEC2C)**

089 As a main-conference extension, we select a sparse subset of token positions to transfer and fuse.
 090 Let $I \subset \{1, \dots, T\}$ be selected tokens and S_I the gather operator. We fuse only selected tokens and
 091 scatter updates back:

$$\begin{aligned} (\tilde{K}_\ell^R, \tilde{V}_\ell^R) &= S_I^\top(K_\ell^R, V_\ell^R), \quad (\tilde{K}_\ell^S, \tilde{V}_\ell^S) = S_I^\top(K_\ell^S, V_\ell^S) \\ (\tilde{K}_\ell^{R'}, \tilde{V}_\ell^{R'}) &= \mathcal{F}_\ell(\tilde{K}_\ell^R, \tilde{V}_\ell^R, \Pi_\ell^K(\tilde{K}_\ell^S), \Pi_\ell^V(\tilde{V}_\ell^S)). \end{aligned}$$

092 We then scatter the update to the full cache. We use projector-aware token scoring by computing
 093 value norms in receiver space (`proj_vnorm_topk`), tying selection to the cross-model mapping.

108 4.4.1 RECEIVER-AWARE DELTA SELECTION (M9)
109110 For sparse transfer, the receiver already has a cache baseline, so sending large-but-redundant tokens
111 wastes bandwidth. We score each token by its *marginal update* in receiver space:

112
$$\Delta V_t^\ell = \widehat{V}_{:,:,t,:}^\ell - V_{:,:,t,:}^{R,\ell}, \quad u^\ell(t) = \mathbb{E}_{b,h} [\|\Delta V_{b,h,t}^\ell\|_2].$$

113

114 We select the top- k tokens by $u^\ell(t)$ under a token budget $|I_\ell| \leq \lfloor pT \rfloor$:

115
$$I_\ell = \text{TopK}(u^\ell(t); \lfloor pT \rfloor).$$

116 This `delta_proj_vnorm_topk` score is projector-aware and redundancy-aware by construction.
117118 4.4.2 RATE-DISTORTION TOKEN×PRECISION SCHEDULING (M10)
119120 Under a fixed communication budget, we jointly select tokens and precisions. Each token t chooses
121 an action $a_t \in \{\text{drop, int4, int8}\}$ with rate $r(a_t)$ (bits/element). We minimize distortion under a byte
122 budget:

123
$$\min_{a_t} \sum_t D_t(a_t) \quad \text{s.t.} \quad \sum_t r(a_t) \leq R_{\text{budget}},$$

124

125 with $D_t(\text{drop}) = \|\widehat{V}_t - V_t^R\|_2^2$ and $D_t(\text{intb}) = \|\widehat{V}_t - \widehat{V}_t^{(\text{intb})}\|_2^2$. We implement a deterministic greedy
126 allocator (RD-Greedy) that assigns INT8 to highest-utility tokens, then INT4, then drop, until the
127 byte budget is met.128 4.5 COMMUNICATION-BUDGET CURVES
129130 We report accuracy as a function of transmitted bytes, enabling fair comparison under equal com-
131 munication constraints. For a sequence of length T , the approximate bytes are
132

133
$$\text{bytes} \approx T \cdot p \cdot 2 \cdot L \cdot H_{kv} \cdot d_h \cdot b/8,$$

134 where p is the retained cache proportion, L the number of layers, H_{kv} KV heads, d_h head dim, and
135 b bits per element. We use this accounting for consistent budget curves.
136137 5 EXPERIMENTS
138139 5.1 SETUP
140141 We evaluate on OpenBookQA and ARC-C with a Qwen3-0.6B receiver and Qwen2.5-0.5B sharer.
142 We follow the C2C eval protocol: temperature 0, max_new_tokens 64, no CoT, unified chat template.
143 All models are frozen; only the projector is trained when QAT is enabled. The OpenBookQA test
144 split has 500 samples and ARC-C has 1150 samples.145 5.2 MAIN RESULTS
146147 All results below are full runs. PTQ is effectively lossless relative to FP16, and cache pruning shows
148 a strong front/back asymmetry.
149150 151 **Table 1: Baseline vs. PTQ (full-cache, %).**

| Setting | OpenBookQA | ARC-C |
|---------------|------------|-------|
| FP16 baseline | 52.8 | 55.1 |
| INT8 PTQ | 52.8 | 55.0 |
| INT4 PTQ | 52.6 | 55.4 |

152 5.3 COMMUNICATION-BUDGET CURVE
153154 Figure 1 and Figure 2 report accuracy versus effective transmitted bytes. Each point is annotated
155 with the retained cache proportion. These curves provide a single, comparable view across precision
156 (FP16/INT8/INT4) and cache-length reduction.
157

162
163
164
165
166
167
168
169
170
171
172
173
174
175

Table 2: OpenBookQA accuracy (%), 500 samples) for cache-length pruning (INT8).

| Order mode | 75% | 50% | 25% | 10% |
|------------|------|------|------|------|
| Front | 44.6 | 43.0 | 38.8 | 38.6 |
| Back | 52.2 | 52.0 | 50.8 | 49.2 |

Table 3: ARC-C accuracy (%), 1150 samples) for cache-length pruning (INT8).

| Order mode | 75% | 50% | 25% | 10% |
|------------|------|------|------|------|
| Front | 40.2 | 46.3 | 38.3 | 40.7 |
| Back | 55.7 | 57.2 | 56.2 | 53.7 |

5.4 ORDER-MODE ABLATION

Across all cache lengths, **back-pruning** (keeping later instruction tokens) consistently outperforms **front-pruning**. At 50% cache length, for example, back-pruning retains near-baseline accuracy while front-pruning degrades sharply. This suggests late instruction tokens carry higher utility for cross-model KV fusion, a useful design signal for future selective transfer methods.

5.5 RECEIVER-AWARE SELECTION AND RD SCHEDULING

We compare M9 delta selection against value-norm baselines at a fixed token budget ($p = 0.25$, INT8, prompt-only). Delta selection improves accuracy over both vnorm and proj_vnorm heuristics on both datasets (Table 4).

Table 4: M9 selection at $p = 0.25$ (INT8, base pair).

| Token selector | OpenBookQA | ARC-C |
|-----------------------|-------------|-------------|
| vnorm.topk | 47.0 | 49.6 |
| proj_vnorm.topk | 46.2 | 52.6 |
| delta_proj_vnorm.topk | 49.8 | 54.8 |

RD scheduling provides an additional budget axis. At 1/16 and 1/8 byte budgets, mixed-precision RD (drop+int4+int8) matches or slightly improves over drop+int8 (Table 5), indicating that token-level precision allocation is competitive under tight budgets.

5.6 HETEROGENEOUS PAIR SPOT CHECK

On a heterogeneous pair (Qwen3→Llama3.2, alignment on), M9 delta selection and M10 RD scheduling remain viable (Table 6).

5.7 SYSTEM METRICS

We report end-to-end evaluation time on a single H100 with timing synchronization enabled. M10 incurs additional overhead from token×precision scheduling relative to M9 (Table 7).

5.8 ADDITIONAL EXTENSIONS

Mixed precision (INT8 with FP16 in the last layers) remains near baseline across last-2/last-4/last-8 schedules. Projector-only QAT (INT8) currently degrades accuracy (39.6/40.2), indicating that longer training or recipe tuning is needed. An alignment-only ablation (same model pair, alignment enabled) reduces accuracy, suggesting alignment should be reserved for heterogeneous pairs.

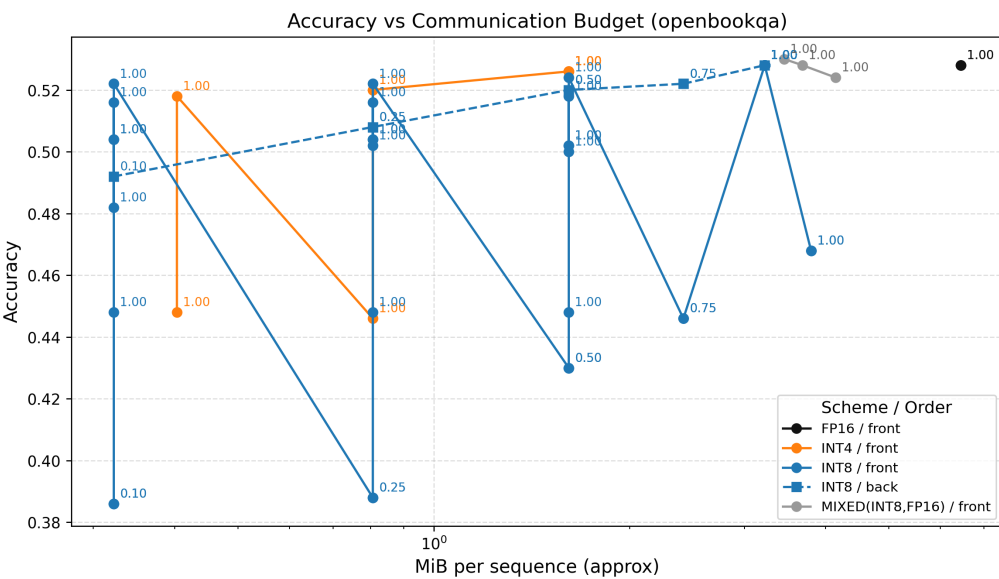


Figure 1: Accuracy vs. communication budget (OpenBookQA).

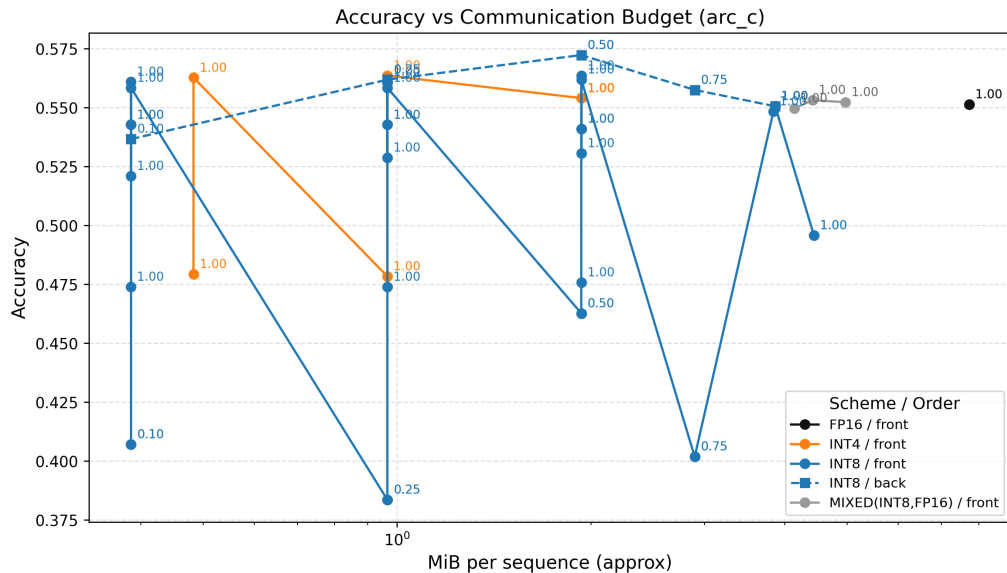


Figure 2: Accuracy vs. communication budget (ARC-C).

GSM8K with CoT. On GSM8K, CoT prompting remains challenging at this model scale. M10 RD (1/8 budget) improves accuracy over M9 delta ($p=0.25$) by +0.014 absolute (0.042 vs 0.028), but both are far below competitive levels.

6 DISCUSSION

Quantized C2C provides large bandwidth reductions with limited accuracy drop. Receiver-aware delta selection consistently improves low-budget accuracy, and RD-C2C achieves near-baseline performance at moderate byte budgets. Shard-based repeats show low variance ($\text{std} \leq 0.02$), supporting robustness at tight budgets. Timing-sync measurements indicate RD scheduling adds overhead rel-

270

271 Table 5: M10 RD ablation (base pair).

| Setting | OpenBookQA | ARC-C |
|--------------------------|-------------|-------|
| RD 1/16 (drop+int8) | 52.6 | 57.2 |
| RD 1/16 (drop+int4+int8) | 53.4 | 57.0 |
| RD 1/8 (drop+int8) | 52.4 | 54.9 |
| RD 1/8 (drop+int4+int8) | 52.4 | 54.9 |

272

273

274

275

276

277

278

279

280

281

282

283

284

285

286

287

288

289

290

ative to delta selection, highlighting the compute–communication tradeoff. A main-conference path includes QAT recovery, broader heterogeneity, and more system-level profiling beyond single-GPU eval time.

7 LIMITATIONS

Our results focus on a single base pair and two primary datasets; heterogeneity is evaluated via a single spot check. Timing-sync evals capture end-to-end runtime on a single GPU but do not measure distributed communication overhead or kernel-level profiling. GSM8K remains challenging: with CoT enabled, M10 improves over M9 but overall accuracy is still low. These limitations will be addressed in the final main-conference revision.

8 BROADER IMPACT

Communication-efficient multi-LLM systems can reduce compute and latency, but they may also enable higher-throughput deployment of models. We emphasize reproducible evaluation, careful reporting of accuracy/latency tradeoffs, and responsible deployment in sensitive domains.

9 CONCLUSION

We introduce precision-aware C2C and report accuracy vs. bytes curves. This establishes a communication-budget perspective for cross-model KV transfer and opens the door to low-latency, low-bandwidth agent collaboration.

ACKNOWLEDGMENTS

Placeholder.

REFERENCES

- Anonymous. Attention score is not all you need for token importance indicator in kv cache reduction: Value also matters. 2024a.
- Anonymous. Zipcache: Accurate and efficient kv cache compression for llm inference. 2024b.
- Anonymous. Tokenselect: Efficient long-context inference with token-level kv cache selection. 2025.
- Lucio M. Dery, Zohar Yahav, Henry Prior, Qixuan Feng, Jiajun Shen, and Arthur Szlam. Latent space communication via k-v cache alignment. 2026.

324
325
326
327
328
329
330
331
332
333
334
335
336
337
338
339
340
341
342
343
344
345
346
347
348
349
350
351
352
353
354
355
356
357
358
359
360
361
362
363
364
365
366
367
368
369
370
371
372
373
374
375
376
377

Table 7: End-to-end timing (seconds; per-sample in parentheses).

| Setting | OpenBookQA (500) | ARC-C (1150) |
|-------------------|------------------|---------------|
| M9 delta (p=0.25) | 279.5 (0.56) | 675.1 (0.59) |
| M10 RD (1/8) | 412.2 (0.82) | 1056.9 (0.92) |

Table 8: Additional extension results (% accuracy).

| Setting | OpenBookQA | ARC-C |
|--|------------|-------|
| Mixed precision (INT8 + last-2 FP16) | 53.0 | 55.0 |
| Mixed precision (INT8 + last-4 FP16) | 52.8 | 55.3 |
| Mixed precision (INT8 + last-8 FP16) | 52.4 | 55.2 |
| QAT (projector-only, INT8) | 39.6 | 40.2 |
| Alignment ablation (same pair) | 46.8 | 49.6 |
| Hetero pair (Qwen3→Llama3.2, align on) | 44.2 | 47.8 |

Tianyu Fu, Zihan Min, Hanling Zhang, Jichao Yan, Guohao Dai, Wanli Ouyang, and Yu Wang.
 Cache-to-cache: Direct semantic communication between large language models. 2025.

Boris Kriuk and Logic Ng. Q-kvcomm: Efficient multi-agent communication via adaptive kv cache compression. 2025.

Hancheng Ye, Zhengqi Gao, Mingyuan Ma, Qinsi Wang, Yuzhe Fu, Ming-Yu Chung, Yueqian Lin, Zhijian Liu, Jianyi Zhang, Danyang Zhuo, and Yiran Chen. Kvcomm: Online cross-context kv-cache communication for efficient llm-based multi-agent systems. 2025.

Jiaru Zou, Xiyuan Yang, Ruizhong Qiu, Gaotang Li, Katherine Tieu, Pan Lu, Ke Shen, Hanghang Tong, Yejin Choi, Jingrui He, James Zou, Mengdi Wang, and Ling Yang. Latent collaboration in multi-agent systems. 2025.